RESEARCH ARTICLE SUMMARY

ECOLOGY

Exit time as a measure of ecological resilience

Babak M. S. Arani, Stephen R. Carpenter, Leo Lahti, Egbert H. van Nes*, Marten Scheffer*

INTRODUCTION: Financial markets may collapse, rainforest can shift to savanna, a person can become trapped in a depression, and the Gulf Stream can come to a standstill. Such critical transitions may happen in complex systems when resilience is low, allowing a perturbation to trigger self-propelled change toward the contrasting state. An intuitive way of visualizing this is to depict the system as a marble in a cup. If the cup is shallower, resilience is lower, and it becomes easier to flip the marble out. Resilience may sometimes be inferred from autocorrelation and variance of time series because they carry information about recovery rates from small perturbations, thus reflecting the slope of the attraction basin. However, although differences in such indicators may reflect differences in resilience, they cannot be interpreted in an absolute sense. The alternative—measuring resilience as the maximum perturbation that a system can take—may seem more attractive. However, this classical ecological definition of resilience assumes that the system is affected by distinct, isolated perturbations. In reality, most systems are perturbed instead by a never-ending natural regime of shocks and fluctuations. Thus, they rarely recover from a perturbation before the next one comes. As a result, the imaginary marble in the cup keeps wandering around, and occasionally a sequence of small but synergistic "perturbations" will push the system across the border of the basin of attraction. How then can we characterize the resilience of such systems in a useful and practical way?

RATIONALE: We propose to use "life expectancy" as a measure of resilience, which can be formalized as the mean exit time from an attraction basin (i.e., the expected time required to cross the border of the basin). This approach has the advantage of taking the natural variability of real complex systems explicitly into account. If we have many observations of shifts, we can calculate the mean exit time simply as the average time the system spends in each given state. However, such data are rare. Moreover, the permanent fluctuations also contain information about the system, which would be lost if one considers only the rare occasions at which a shift occurs. In the approach we outline, this information is used as we infer the deterministic and stochastic components of the underlying dynamical system from observed fluctuations. Applying techniques from statistical mechanics, we show how one can subsequently use the reconstructed empirical model to compute the expected mean exit time for each basin of attraction.

RESULTS: After using model-generated data to demonstrate the method, we applied it to two examples spanning very different time scales: the rapid dynamics of Cyanobacteria in a lake, and the much slower alternations between cold glacial and warmer interstadial regimes in the climate (the so-called Dansgaard-Oeschger events). For both time series, we show that one can reconstruct a model that has two alternative attractors. We estimated the mean exit time for each of these attractors, and we show how one can analyze the uncertainty of this estimate.

A major challenge is that the approach requires high-resolution time series that cover dynamics across both basins of attraction. Such information can be obtained from a single long time series if it includes enough shifts between attraction basins. Alternatively, one may piece the required data together using shorter time series from sets of similar systems.

CONCLUSION: Characterizing resilience as the estimated life expectancy—of a rainforest, a coral reef, or the thermohaline circulation—is a natural and intuitively straightforward way to go. The high-resolution time series required for the approach we outline are still relatively rare. However, possibilities for automated sensing are rapidly expanding in fields as diverse as biomedicine, climate science, ecology, and financial markets. Against this background, the technique for estimating mean exit times is an exciting additional tool to anticipate critical transitions in the many complex systems on which humanity depends. ■

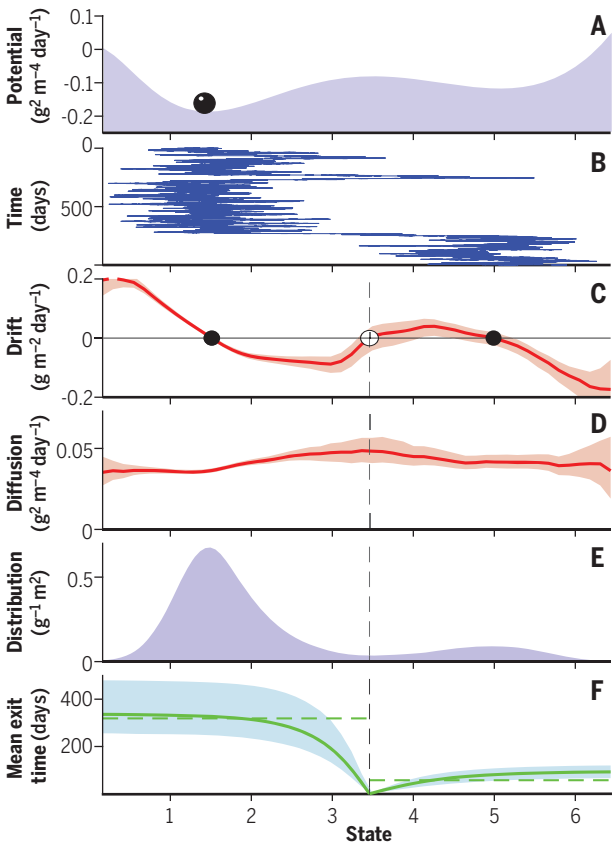

Mean exit time as a measure of "life expectancy" estimated from fluctuations. Time series in this simulated example (**B**) reflect the underlying stability landscape (**A**) as well as the regime of stochastic perturbations. Given sufficiently long time series, we can estimate how the average change depends on the state (**C**), revealing attracting (black dots) and repelling (open dot) equilibria. Meanwhile, variance in the observed change allows estimation of the role of stochasticity (**D**). The resulting empirical model [based on (C) and (D)] can be used to compute the probability distribution of states (**E**), the mean exit time given any initial state (**F**), and the weighted mean exit time for the alternative basins of attraction [horizontal lines in (F)]. The shaded areas in (C), (D), and (F) are the estimated 95% confidence intervals.

The list of author affiliations is available in the full article online.
*Corresponding author. Email: marten.scheffer@wur.nl (M.S.); egbert.vannes@wur.nl (E.H.v.N.)
Cite this article as B. M. S. Arani *et al.*, *Science* **372**, eaay4895 (2021). DOI: 10.1126/science.aay4895

S READ THE FULL ARTICLE AT
https://doi.org/10.1126/science.aay4895

Downloaded from https://www.science.org at University of British Columbia on September 10, 2021

RESEARCH ARTICLE

ECOLOGY

Exit time as a measure of ecological resilience

Babak M. S. Arani[1,2], Stephen R. Carpenter[3], Leo Lahti[4], Egbert H. van Nes[1]*, Marten Scheffer[1]*

Ecological resilience is the magnitude of the largest perturbation from which a system can still recover to its original state. However, a transition into another state may often be invoked by a series of minor synergistic perturbations rather than a single big one. We show how resilience can be estimated in terms of average life expectancy, accounting for this natural regime of variability. We use time series to fit a model that captures the stochastic as well as the deterministic components. The model is then used to estimate the mean exit time from the basin of attraction. This approach offers a fresh angle to anticipating the chance of a critical transition at a time when high-resolution time series are becoming increasingly available.

Ecosystems occasionally undergo a catastrophic shift to a contrasting state from which recovery is difficult (*1*). For instance, tropical forests may shift to a fire-dominated savanna state (*2*, *3*), coral reefs may become overgrown by macroalgae (*4*), and lakes can shift between a clear and a turbid state (*5*, *6*). Such critical transitions are not limited to ecology (*7*). For instance, some humans may shift into a depressed state (*8*), financial markets sometimes collapse (*9*), and elements of Earth's climate system such as ocean circulation patterns may shift between contrasting modes (*10*). In view of the societal impact of such critical transitions, there is a broad interest in anticipating them (*11*). An influential approach is to focus on resilience, defined as the magnitude of perturbations that a system can withstand and still maintain its essential characteristics in terms of composition and functioning (*12*). This way of viewing resilience originated in ecology (*13*) but has become influential in a wide range of fields including human and animal health (*8*, *14*, *15*), climate science (*10*, *16*), and the social sciences (*17*, *18*). An attractive and widespread way of visualizing this concept of resilience is to depict the system as a marble in a cup. If the cup becomes shallower or narrower (*13*), it becomes easier to flip the marble out. Indeed, in many situations, loss of resilience can be intuitively understood as shrinkage of a basin of attraction (the cup). However, quantifying resilience in practice remains challenging.

One approach has been to estimate changes in recovery rate from small perturbations as an indicator of changes in the overall size of the attraction basin. The basic idea is that the slowing down of such recoveries is an indicator of loss of resilience, and thus an increased risk of being flipped out of the basin of attraction by some perturbation (*19*–*21*). Such slowing down can be probed by experimental perturbations but can also be inferred from natural time series, where it can be reflected in indicators such as rising temporal autocorrelation and variance (*20*, *22*, *23*). A major limitation of such dynamic indicators of resilience is that they can only be interpreted in a relative sense, to infer rising or falling trends in time or compare between different instances of a system (e.g., ranking resilience of different patients, forests, or reefs) (*20*, *22*, *23*). By contrast, resilience quantified as the maximum perturbation that a system can take without flipping into an alternative state can be expressed in absolute terms (e.g., the

[1]Aquatic Ecology and Water Quality Management, Wageningen University, 6700 AA Wageningen, Netherlands. [2]Theoretical Research in Evolutionary Life Sciences, Groningen Institute for Evolutionary Life Sciences, University of Groningen, 9700 CC Groningen, Netherlands. [3]Center for Limnology, University of Wisconsin, Madison, WI 53706, USA. [4]Department of Computing, University of Turku, Turku, Finland.
*Corresponding author. Email: marten.scheffer@wur.nl (M.S.); egbert.vannes@wur.nl (E.H.v.N.)

Downloaded from https://www.science.org at University of British Columbia on September 10, 2021

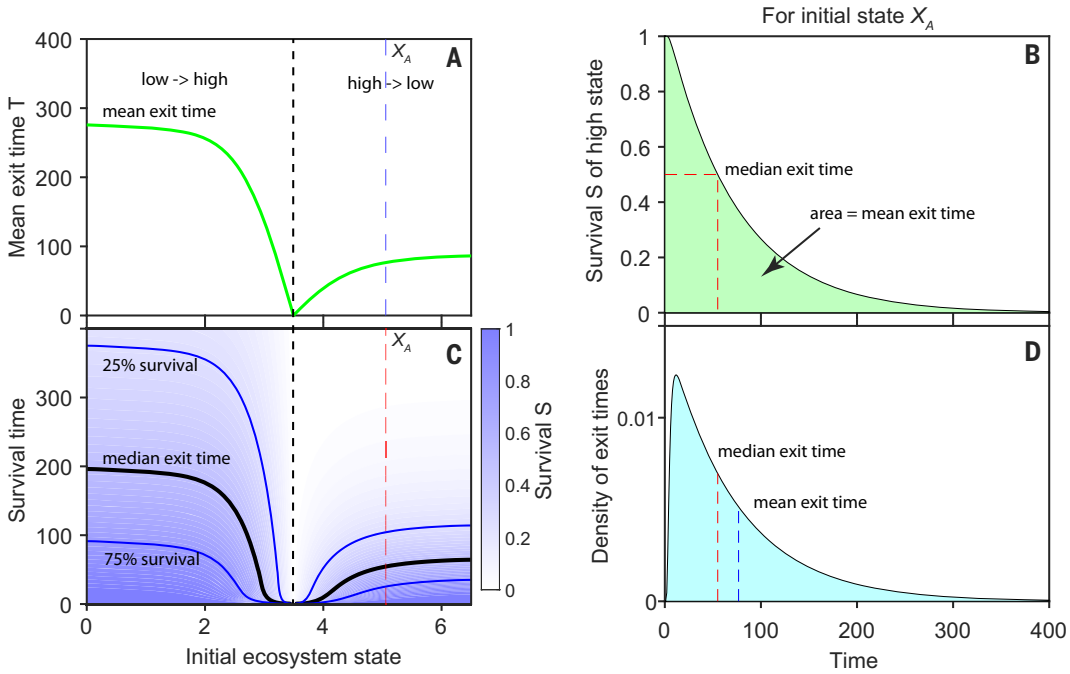

Fig. 1. Different ways of representing the exit time in a system with two alternative basins of attraction (Eq. 4). (**A**) Mean exit time as a function of the initial state. The dashed black line marks the border between the two basins of attraction. The left and right sides of the plot show the exit time from the low-biomass and high-biomass basins of attraction, respectively. (**B**) The survival fraction as a function of the elapsed time for a given initial state X_A [indicated in (A) and (C) as vertical dashed blue and red lines]. At the median survival time (= median exit time), 50% of the trajectories shift from the high state to the low state. The green area below the curve equals the mean exit time. (**C**) The survival function $S(x_0,t)$ can be depicted as the fraction of trajectories remaining in the original basin of attraction after a given time depending on the initial state. Contours where 25%, 50%, and 75% of the trajectories survive are indicated. Note that 50% survival equals the median exit time. (**D**) The negative of the derivative of the survival function (B) equals the distribution of exit times of the state X_A. Median and mean exit times are indicated. Parameters: a = 1.6, γ = 2.75, K = 10, r = 1, σ = 0.3.

number of elephants to be culled while remaining a viable population). However, appealing as it seems, this classical ecological definition of resilience has another crucial drawback: It assumes that the system is affected by distinct, isolated perturbations. Clearly, thinking in terms of such isolated perturbations is in fact artificial. In reality, there is typically a continuous interplay of internal and external fluctuating forces affecting the system (24), and it makes more sense to try to capture the essence of this whole complex of deterministic and stochastic forces (25) instead of an imaginary stable system exposed to discrete external perturbations. This is especially so because a system may rarely recover from a perturbation before the next one comes. As a result, the imaginary marble in the cup keeps wandering around, and it is easy to imagine how occasionally a sequence of small but synergistic "perturbations" will push the system across the border of the basin of attraction. To get a better feel for why the single-perturbation view is inadequate, see movie S1.

If the attractive view of a bistable system perturbed by occasional extreme events is too simple, how then may we characterize the resilience of such systems in a more useful way? As we will show, an attractive option is to estimate the "mean exit time" (26, 27). This measure corresponds to the expected time it takes for the system to cross a threshold such as the border of an attraction basin. It corresponds in an intuitively straightforward way to the expected "survival time," which is analogous to the way we think about life and death. Clearly, considering the expected survival time of a rainforest, a coral reef, or the thermohaline circulation makes things more concrete and intuitive than mere estimation of relative differences in resilience. However, estimating the mean exit time is not trivial, and in ecology it is only applied in models (27, 28). If we have many observations of shifts across a defined threshold, we can calculate the mean exit time directly by simply averaging the periods during which the system is within a given range before passing the threshold. However, often such repeated crossings are not observed. Moreover, there is information in the permanent fluctuations of a system that would be lost if one considers only the rare occasions at which a threshold is crossed. A way to use this information is to fit a so-called Langevin equation to a time series, capturing the essence of the dynamics, and subsequently estimate the mean exit time from this fitted model. Below, we explain how this works in a nutshell and give some examples. An extensive glossary (29) explains the key concepts in more detail.

The approach in a nutshell

The one-dimensional Langevin equation, used to capture the essence of a time series for our purpose, describes the dynamics of a single state variable (x):

$$dx = f(x)dt + \sigma(x)dW \qquad (1)$$

The function $f(x)$ represents the deterministic part of the equation, representing (for instance) how growth and losses in a population vary with the state. The term dW represents the increments of a Wiener process with uncorrelated random fluctuations following a standard Gaussian distribution. The function $\sigma(x)$ describes how the standard deviation of this "noise" varies with the state. If the functions $f(x)$ and $\sigma(x)$ are known, we can use them to determine the mean exit time by performing long runs and analyzing how frequently the system passes a critical threshold (e.g., the border of the basin of attraction). However, there is also a much more efficient method (26, 30) that describes the system in an

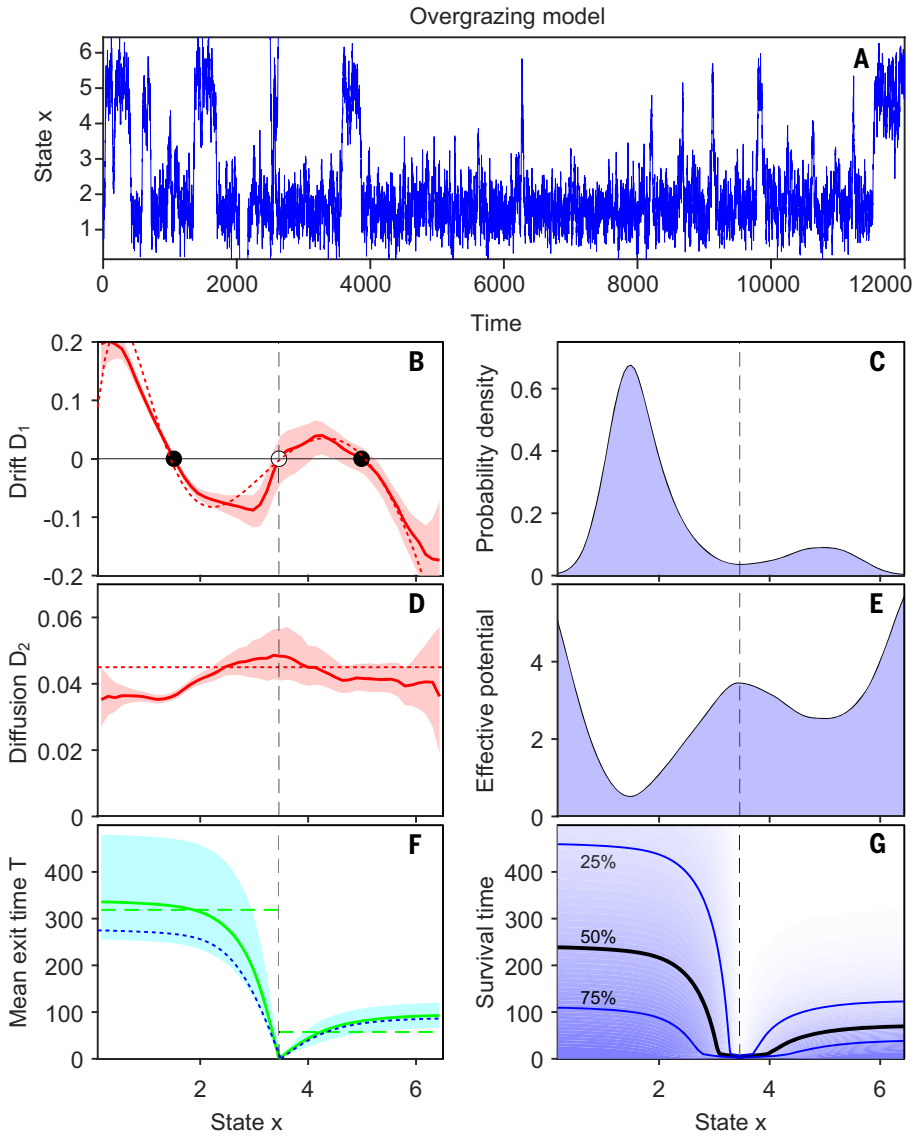

Fig. 2. Illustration of the computation of exit times based on model-generated data (Eq. 4) using the Langevin approach to reconstruct its deterministic and stochastic components. (**A**) The model-generated time series. (**B**) The fitted deterministic drift function D_1 (red solid line) together with the "true" function from the underlying model (red dashed line). (**C**) Expected long-term probability density function. (**D**) The fitted diffusion function D_2 (red line) and the true diffusion function of the underlying model (horizontal dashed line). (**E**) The effective potential landscape. (**F**) The mean exit time of the reconstructed Langevin model (green line) and of the original model (blue dashed line) and the weighted estimated mean exit time of each basin of attraction (dashed green line). (**G**) The survival probability of each attractor of the reconstructed model, starting at different initial states x_0. Indicated are the times where 75%, 50%, and 25% of the trajectories survive (lower, middle, and top lines, respectively). Parameters are as in Fig. 1. The shaded bands in (B), (D), and (F) represent the 95% confidence limits determined with Monte Carlo error propagation based on 1000 pseudo-datasets.

Downloaded from https://www.science.org at University of British Columbia on September 10, 2021

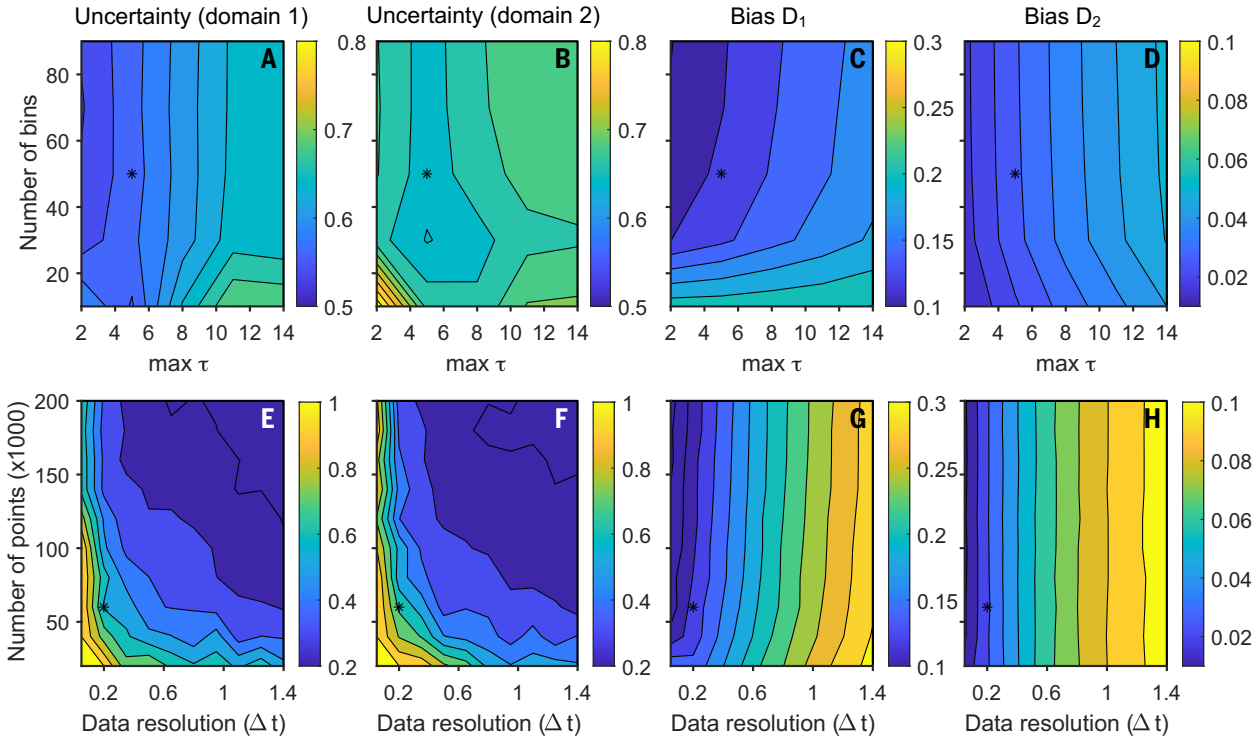

Fig. 3. Sensitivity analysis of the uncertainty in the mean exit time of each domain and the bias in the determination of drift D_1 and diffusion D_2. (**A** to **D**) Effect of number of bins and maximum time lag (τ). (**E** to **H**) Effect of data resolution and number of points of the generated data. The uncertainty of the weighted mean exit time in each of the domains [(A), (B), (E), (F)] is expressed as the relative confidence interval; the bias is the median difference between the drift and diffusion of the reconstructed models and their parent model (*29*). The asterisks indicate the settings used in Fig. 2.

alternative but equivalent way. Instead of following the time evolution of single stochastic runs, this approach generalizes the macroscopic behavior of diffusing particles. From the so-called backward Fokker-Planck equation (*26*), a formula for the direct calculation of the mean exit time $T(x_0)$ can be derived (Eq. 2). The mean exit time is the average time it takes for a trajectory to leave a defined basin of attraction for the first time, starting from a certain initial state x_0 (*26*, *30*):

$$D_1(x_0)\frac{dT}{dx_0} + D_2(x_0)\frac{d^2T}{dx_0{}^2} = -1 \qquad (2)$$

In this equation $D_1(x_0)$ is known as the "drift," which is equal to $f(x_0)$ in the Langevin equation (Eq. 1), and $D_2(x_0)$ is the "diffusion" defined as

$$D_2(x_0) \equiv \frac{1}{2}\sigma(x_0)^2 \qquad (3)$$

where $\sigma(x_0)$ is the noise intensity as defined in the Langevin equation (Eq. 1). Before we solve this boundary value problem (Eq. 2), we have to define the proper boundary conditions for each basin of attraction of Eq. 1. We use "absorbing" boundaries for the unstable edge between two basins of attraction. At this boundary $T(x_0) = 0$, as the exit time is 0 at the border. By contrast, for the other boundaries (left boundary of the left basin; right boundary of the right basin), we use a reflecting boundary to keep the system inside the observed range. This is done by defining $dT/dx_0 = 0$ at the boundary, indicating no change in $T(x_0)$.

Apart from the mean exit time, we can determine various other statistics from the Langevin equation using similar macroscopic descriptions. With a slightly more extended equation (eq. S21), we can describe the survival probabilities as function of the initial conditions and time (Fig. 1, B and C). From this function we can calculate the median exit time (or half-life) and the distribution of exit times. An advantage of using the median exit time is that it is less dependent on the tail of the distribution of exit times. This is important because exit time distribution tends to be right-skewed (*31*–*33*)—a universal feature that can be understood from simple diffusion models (*34*). The consequences become extreme if the distribution of exit times has a fat tail, and no mean value can be computed at all. Similarly, we can use the forward Fokker-Planck equation (eq. S19) to model the time evolution of the distribution of states starting from an initial condition. Often the expected distribution of states stabilizes to a stationary probability density function, which is not dependent on the initial conditions. We can use this stationary distribution to weigh the mean exit times of all initial conditions within a basin of attraction, so as to derive an overall indication of the mean exit time (weighted mean exit time) from a basin of attraction.

Finally, we can determine the effective potential function (eq. S12) from the drift and diffusion functions of the Langevin equation. This "stability landscape" differs from the traditional ones in the sense that it is now not only based on the deterministic part, but also includes effects of state-dependent stochasticity (diffusion). In our examples, we solved the boundary value problem (Eq. 2) in MATLAB using the toolbox of Chebfun (*35*). This MATLAB software is available in (*29*).

From this overview, it should be clear that once we know the drift $D_1(x)$ and diffusion $D_2(x)$ functions, we can determine many statistical properties of the system. The first crucial step in applying this approach in practice is to determine the drift and diffusion functions from data. The "Langevin approach" (*36*–*40*) can determine these functions without prior knowledge about their functional forms. Although the technical details are somewhat complex, involving several steps (*29*, *36*–*40*), the basic idea is straightforward. We estimate $D_1(x)$ and $D_2(x)$ over a binned range of states x to describe these functions. In each of these bins we compute the deterministic part, also called "drift" $D_1(x)$, from the estimated mean rate of change, and the stochastic part, also called "diffusion"

Downloaded from https://www.science.org at University of British Columbia on September 10, 2021

$D_2(x)$, from the estimated variance in the rate of change. After checking whether the resulting Langevin equation successfully describes the data (29), the discretized functions $D_1(x)$ and $D_2(x)$ can be used in the backward Fokker-Planck equation to determine the statistics of exit time. The Langevin equation is also used to estimate the confidence limits of the mean exit time using a Monte Carlo error propagation analysis (29).

Applying the approach to model-generated data

To illustrate how the approach works, we first use it to analyze a time series produced from a stochastic version of a well-known model, describing a plant population (x) that is grazed (41, 42):

$$dx = \left[rx\left(1-\frac{x}{K}\right) - \gamma\frac{x^2}{x^2+a^2}\right] dt + \sigma dW \quad (4)$$

where a is the efficiency of the grazer, γ is the maximum grazing rate, K is the carrying capacity, r is the growth rate, and σ is the size of the additive noise. For suitable parameter settings, this model has alternative basins of attraction: a low-biomass overgrazed state, and a high-biomass undergrazed state where the population escapes top-down control by the consumer. Using the Euler-Maruyama scheme with a time step of 0.001, we ran the model for 12,000 time units (Fig. 2A). From this time series we used 60,000 regularly spaced data points to reconstruct the deterministic and stochastic parts of Eq. 4. Note that although the reconstructed model corresponds relatively well to the original (Fig. 2, B and D), there is a tendency to overestimate the stochasticity close to the unstable point and underestimate it around the attractors. A sensitivity analysis (29) shows that this bias disappears if the model output is sampled at a higher data resolution (43) (Fig. 3, G and H). Despite the tendency to overestimate stochasticity around unstable points, mean exit times correspond closely to what can be derived directly from the original model (Fig. 2F). Using the approach detailed in eq. S12, we can now also compute the effective potential energy landscape accounting for the deterministic as well as the stochastic components (Fig. 2E) and the stationary probability distribution of states (Fig. 2C), which is used to weigh the state-dependent mean exit times to produce an overall weighted mean exit time for the entire basin of attraction (Fig. 2F, horizontal dashed lines). Finally, we can compute survival probabilities as a function of the initial state and time, which can be interpreted as the proportion of trajectories that are still in the basin of attraction after a certain time. This function can be used to determine the median exit time (and other percentiles) and the distribution of exit times (Fig. 1).

Cyanobacterial dynamics as an example of a fast system

We now turn to an example of applying the approach to real data. Our time series consists of estimations of the biomass of Cyanobacteria, measured as concentrations of phycocyanin in Lake Mendota, Wisconsin (44). The phycocyanin concentrations are recorded every minute throughout the year 2011 while the lake surface is ice-free. For our example, we analyzed a period during summer thermal stratification when Cyanobacteria blooms are common (44). There are many transitions between high and low concentrations. The time series exhibits sharp shifts between high and low phycocyanin levels (Fig. 4A). We first confirmed that the data approximately meet the assumptions of the analysis (29), and then estimated the components of the Langevin

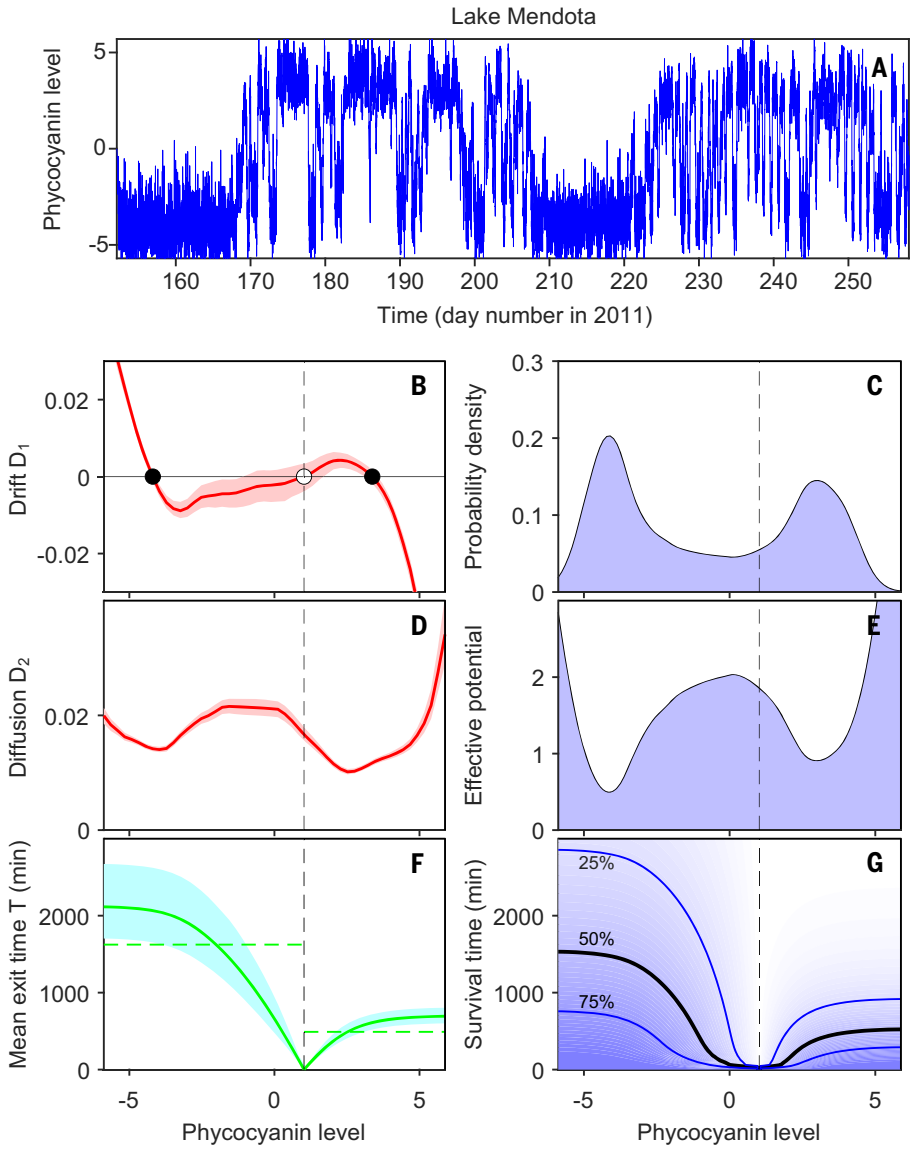

Fig. 4. Resilience of high– and low–cyanobacterial biomass states estimated from phycocyanin concentrations in Lake Mendota in 2011. (**A**) Phycocyanin levels in Lake Mendota computed as the normalized intercepts of a dynamic linear model fitted to log-transformed phycocyanin concentrations (44). (**B**) The fitted deterministic drift function D_1 (red line). (**C**) The expected long-term probability density function. (**D**) The fitted diffusion function D_2 (red line). (**E**) The effective potential landscape of the reconstructed model. (**F**) The mean exit time of the reconstructed model (green line) and the weighted mean exit time of each basin of attraction (dashed green line). (**G**) Survival probability as a function of time of each attractor of the reconstructed model, starting at different initial states x_0. Indicated are the times where 75%, 50%, and 25% of the trajectories survive (lower, middle, and top lines, respectively). Shaded bands in (B), (D), and (F) represent the 95% confidence limits determined with Monte Carlo error propagation based on 1000 pseudo-datasets.

Downloaded from https://www.science.org at University of British Columbia on September 10, 2021

equation (Fig. 4, B and D) (37–40). The drift and diffusion functions were used to compute the effective potential (Fig. 4C) and the stationary probability density (Fig. 4D) (29). The results suggest distinct low and high attractors for phycocyanin levels. We then applied the theory of exit time (29) to compute exit time curves (Fig. 4F) and survival time curves (Fig. 4G) from each basin as a function of the initial state, as well as the weighted mean exit times (Table 1). The relatively short exit times suggest that this system frequently flips back and forth stochastically. We cannot exclude the possibility that spatial heterogeneity contributes to this pattern; there can be high spatial variability in the concentration of Cyanobacteria, with alternative states dominating in different parts of lakes (45). This may contribute to locally sensed dynamics if water masses pass by the sensor that represent dynamics across the two basins of attraction (44).

Table 1. Confidence limits (95%) for the weighted mean exit time from each of the basins of attraction of the different datasets. The confidence limits for the first row are based on 1000 replicate datasets generated by the overgrazing model (Eq. 4) directly. The weighted mean exit times of the left and right basins of the underlying model are 250.9 and 64.8 days, respectively. The other confidence limits are based on reconstructed models (29).

Dataset	Parent model based on	Confidence limits Exit left basin	Confidence limits Exit right basin
None (days)	Model Eq. 4	185 to 351	36.3 to 76.8
Generated by overgrazing model (days)	Single generated dataset	235 to 463	34.0 to 82.8
Lake Mendota phytoplankton (min)	Real dataset	1195 to 2209	389 to 606
Climate (years)	Real dataset	450 to 670	310 to 420

Ancient climate shifts as an example of a slow system

To illustrate the approach for a slower system operating at a much longer time scale, we analyzed an ice-core record that reveals that during the course of the last glaciation—spanning from the end of Eemian interglacial to the beginning of the current Holocene interglacial—the

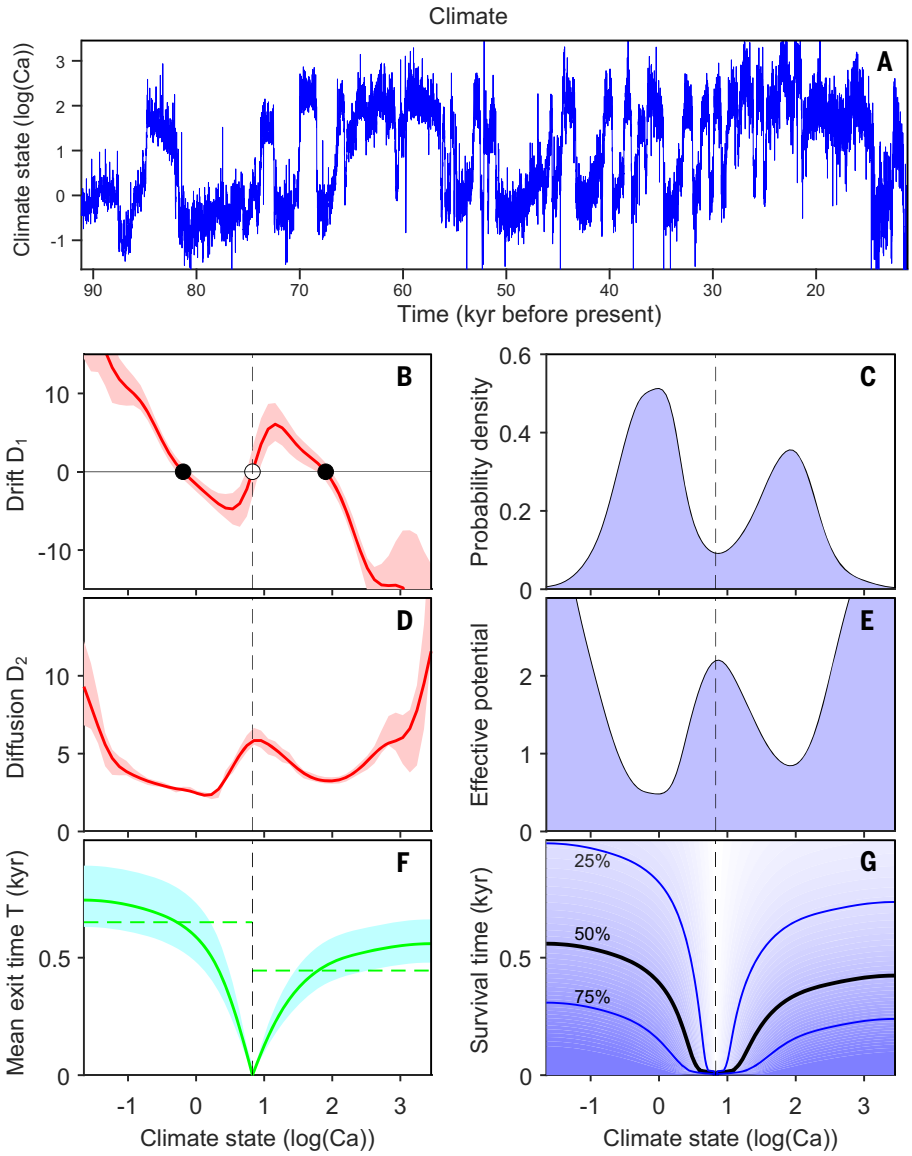

Fig. 5. Resilience of alternative states in the climate system during the last glaciation, as reflected in repeated shifts between colder and warmer states (Dansgaard-Oeschger events). (**A**) Logarithm of calcium concentrations from GRIP ice-core record as a climate proxy. (**B**) The fitted deterministic drift function D_1 (solid red line). (**C**) The expected long-term probability density function. (**D**) The fitted stochastic diffusion function D_2 (red line). (**E**) The effective potential landscape of the reconstructed model. (**F**) The mean exit time of the reconstructed model (green line) and the weighted mean exit time of each basin of attraction (dashed green line). (**G**) The survival probability as a function of time of each attractor of the reconstructed model, starting at different initial states x_0. Indicated are the times where 75%, 50%, and 25% of the trajectories survive (lower, middle, and top lines, respectively). Shaded bands in (B), (D), and (F) represent the 95% confidence limits determined with Monte Carlo error propagation based on 1000 pseudo-datasets.

Downloaded from https://www.science.org at University of British Columbia on September 10, 2021

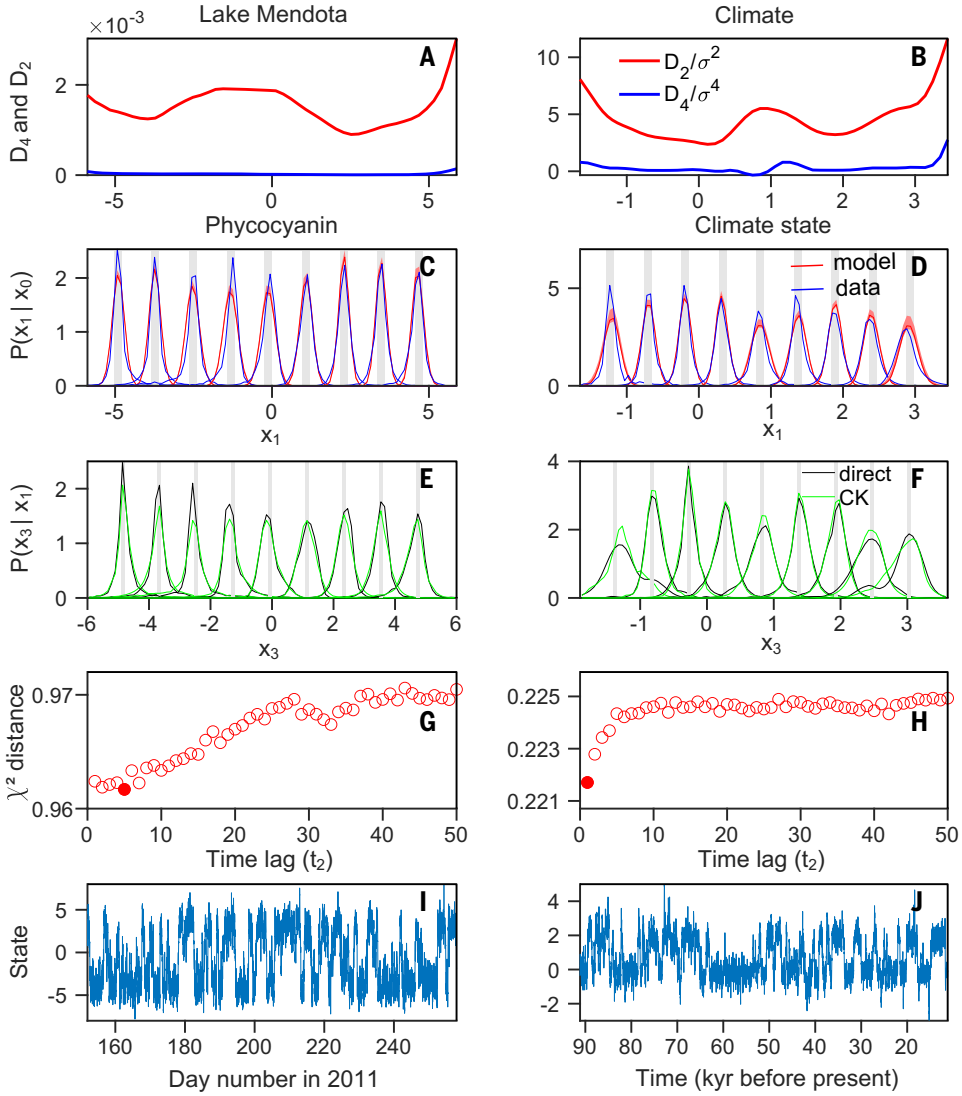

Fig. 6. Data requirements and validation of the Langevin models reconstructed using the phycocyanin data in Lake Mendota (left) and the GRIP climate record (right). (**A** and **B**) The standardized D_4 is small relative to the standardized D_2, which suggests that the process can be described by a drift D_1 and diffusion D_2 term only [Langevin approach, step 3 (*29*)]. (**C** and **D**) One-step conditional probabilities $p(x_1|x_0)$ calculated from the data (blue) and the corresponding reconstructed model (red) for nine evenly distributed x_0 values over the domain (bins indicated as gray bars). The narrow red shaded band is the 95% range of 100 simulated datasets. (**E** and **F**) Comparison between conditional probability distributions obtained from one big step versus two small steps in the time series to assess how well the Markov property holds according to the Chapman-Kolmogorov (CK) equation [Langevin approach, step 1 (*29*)]. (**G** and **H**) The χ^2 distance between the conditional probability density functions such as the ones compared in (E) and (F) as a function of the time lag that is used. The minimum indicates the Markov-Einstein time scale. (**I** and **J**) Examples of simulations with the reconstructed models, to compare with the original time series shown in Figs. 4A and 5A.

climate alternated between cold glacial and warmer interstadial regimes (Fig. 5A), a phenomenon called Dansgaard-Oeschger (DO) events (*46*). Such transitions were a consequence of the reorganization of ocean circulation (*47*) where the stochastic forcing encompasses variations in wind stress, heating, and freshwater transport (*48*). The calcium record from the GRIP (Greenland Ice Core Project) has the highest temporal resolution among ice-core records (*48*) and covers most of the last glaciation and DO events (*49*). This high-resolution dataset approximately meets the conditions for the Langevin approach (*29*). Applying the method, we disentangled the deterministic and stochastic components of the climate system over the last glaciation (Fig. 5, B and D), showing that we can explain the transitions in this period as shifts between alternative stable states. We find that it took, on average, 550 years for the climate system to be tipped from the glacial basin (Fig. 5F, left green line), whereas the backward transition took ~380 years (see Table 1 for confidence intervals). This suggests a rather similar equal resilience for glacial and interstadial climate regimes in the studied period, which is also reflected in the stationary probability density functions (Fig. 5C) and the estimated effective potential function (Fig. 5E).

Discussion

Perhaps the most important advantage of characterizing an expected exit time is that it provides a quantifiable, absolute measure that is easily interpretable as the "life expectancy" of the system state. This is different from the information obtained from potential landscapes, which can also be reconstructed from the distribution of data as illustrated for tropical forests (*2*), the human microbiome (*50*), and the climate system (*51*). The potential landscapes actually look quite similar for alternative attractors in tropical tree cover (*2*) and in abundance of a bacterial group in the human intestine (*50*). However, one cannot deduce the average lifespan of the different states from the static distribution data alone. The size of the alternative basins of attraction contains information about the relative resilience of the two states, but without assumptions about the stochasticity, it cannot reveal the time scale at which shifts may be expected. By contrast, the mean exit time can be directly interpreted in intuitively meaningful ways, which makes it easier to compare different systems.

Another fundamental difference with respect to previous ways of quantifying resilience is that the mean exit time integrates the characteristic stochasticity of a system. Classical representations of resilience focus on the basin of attraction as reflecting the properties of the underlying deterministic system, whereas stochastic perturbations are external. However, one could argue that this separation is artificial. In ecosystems, the natural regime of disturbances (*52*) is an important characteristic, causing them to be in a transient state most of the time (*53*). Indeed, the permanent regime of small disturbances is an important factor that is believed to help

Downloaded from https://www.science.org at University of British Columbia on September 10, 2021

maintain the biodiversity of iconic ecosystems such as coral reefs and tropical forests (54). Another argument against separating internal (deterministic) from external (stochastic) forces is that a substantial part of the "disturbances" may originate from within the system. For instance, forest fires are dependent not only on external conditions such as drought or lightning, but also on the fuel generated by the forest itself. Stochasticity can also be fully internal, such as that caused by demographic noise (55) in small populations. Clearly, separating stochastic drivers from clean deterministic processes makes little sense in such situations. The way in which deterministic dynamics may bring a system across the boundary of the attraction basin is well understood in the field of bifurcation analysis (56). However, in noisy environments, such behavior rapidly becomes much more complex (57, 58). In practice, ecological fluctuations are typically driven by a complex interplay of such internal dynamics and the effects of forcing by climatic dynamics (24) involving intricate resonance phenomena (59, 60) that make it impossible to distinguish which part of the fluctuations should be ascribed to internal versus external mechanisms (7). In view of this entanglement, it is natural to embrace stochasticity as an intrinsic part of the system, responsible in part for shaping the likelihood of a critical transition into another basin of attraction.

Although the mean exit time is a realistic and intuitive measure of resilience, estimating it from data remains a challenge; it can only be determined in a meaningful way if various transitions have been observed. This implies that the data series needs to be sufficiently long. Moreover, if the resolution is not fine enough, the Langevin approach will be biased and may, for instance, overestimate the role of stochasticity in the vicinity of the unstable equilibrium separating the basins of attraction (see Fig. 3). In that situation, we can use survival analysis (61) as an alternative to estimate the mean exit time. Recently, other advanced ways to reconstruct the Langevin equation from data have been proposed [reviewed in (62)], but these methods require equidistant data at even higher resolution. Data requirements thus remain a central limitation.

There are also more fundamental issues. The Langevin equation, like any other model, is a simplification of reality. The question is not whether such models faithfully describe reality, but rather whether the simplification retains enough of the essence to be useful. Strictly speaking, we need the system to be stationary (i.e., with constant statistical properties) and Markovian (the future state depends only on the present state). The latter implies that the system is driven by white noise (without time correlation). In our examples, these properties are approximately fulfilled [Fig. 6, E to H, and tests in (29)], but none of them is likely to be fully true in any real situation. It seems unlikely that the characteristics of the climate system remain unaltered over any long timespan. Weather, a key driver of any ecosystem, is always autocorrelated, and slow system components (such as ice caps for the climate, or soils for ecosystems) imply a long memory on which the faster dynamics are superimposed.

Dimensionality is another fundamental challenge. Complex systems are by definition composed of many interacting elements. In systems such as coral reefs, it is in practice impossible to measure all these dimensions, and we have to focus on a few compound measurable variables and treat the overall effect of fast unobserved variables as noise (63).

Although the Langevin method can in principle be applied to more than one dimension, the requirement for binning in all dimensions exponentially inflates data requirements (64). Clearly, representations of complex systems through a single variable should be interpreted with care (65). On the other hand, a single well-chosen variable can capture much of the essential information when it comes to understanding critical transitions (2, 66). For instance, although the climate system is highly multidimensional, a surprisingly large proportion of millions of years' worth of global climate dynamics is reflected in the variation of $\delta^{18}O$ concentration along a Greenland ice core, and as the system approached a tipping point for abrupt deglaciation, fluctuations in this $\delta^{18}O$ reflect a critical slowdown that signals the upcoming instability (66). Similarly, although rainforest dynamics involve a tremendously complex network of interacting species of plants and animals, indicators of critical slowing down in fluctuations of remotely sensed greenness can indicate dwindling resilience (67).

Challenges of high dimensionality and requirements of stationarity and Markovianity imply that the Langevin approach cannot be more than an approximation. The question is whether that approximation is good enough to be useful. One way to validate the model is by checking whether datasets generated with the fitted models and the corresponding original data have the same statistical properties (Fig. 6, A, B, G, and H). Another way to check robustness is to compare the results to those from the straightforward survival time analysis (61) (Fig. 7). One simply quantifies how long the system tends to "survive" in a particular state. This requires observations covering large number of shifts out of the state, but even with limited data, one can still use the outcome

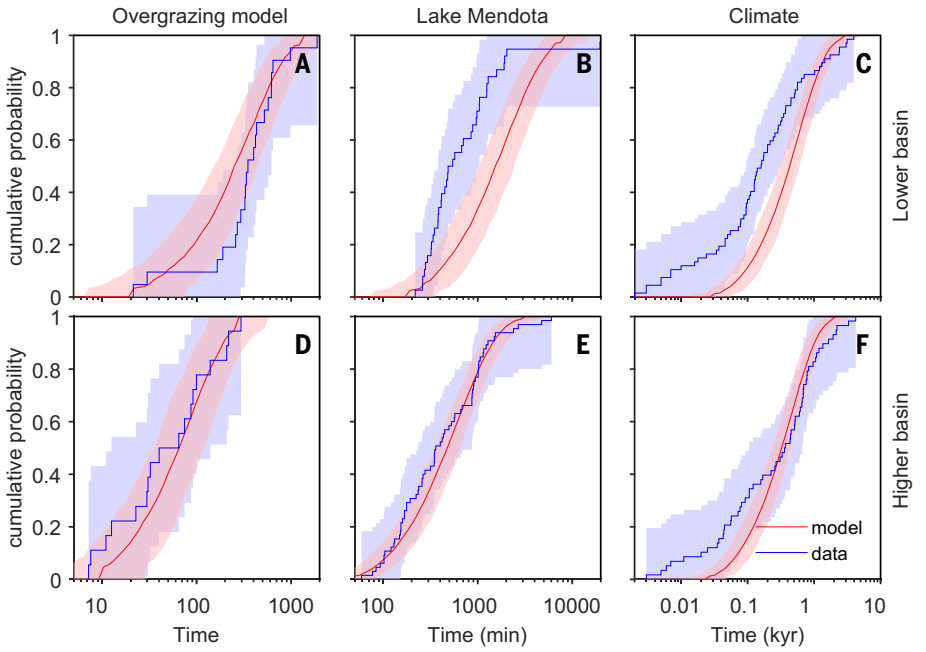

Fig. 7. Comparison of cumulative distributions of the exit times determined directly from the original data (blue) versus data simulated from the corresponding Langevin equations (red). Here, exit time is defined as the time it takes to reach the basin boundary from each of the stable states. The blue shadings are the 95% confidence bounds using the Dvoretzky-Kiefer-Wolfowitz-Massart approach (77, 78). To compare with the resulting models, we also determined the mean exit times in the same way in 1000 generated datasets of the reconstructed models (datasets with random initial conditions and the same size and resolution as the original datasets). The red lines are the medians of the found cumulative distributions; the red shading indicates the 2.5% and 97.5% percentiles of the cumulative distributions from the 1000 generated datasets.

Downloaded from https://www.science.org at University of British Columbia on September 10, 2021

to roughly check the results from a Langevin approach. Finally, one may use frequency distributions of the state of a system to estimate the potential function (*51*), assuming Gaussian white noise. If it is possible to characterize the stochasticity separately, one may estimate the mean exit time using the Arrhenius law or a more refined formula (*68*, *69*). Such cross-comparisons can help in analyses of the outcomes of the Langevin approach that inevitably rely on simplifying assumptions and may vary depending on methodological choices (*29*).

Prospects

The approach we have illustrated enriches the toolkit for inferring the dynamical properties of complex systems from time series of observations. It estimates the expected lifetime of alternative states, embracing stochasticity as an intrinsic characteristic rather than artificially separating it out as purely external. A challenge for practical application of the approach is that it requires long, high-resolution time series that cover dynamics across both basins of attraction to enable estimation of the drift and diffusion functions. Such information can be obtained from a single long time series if it includes enough shifts between attraction basins, but such time series have traditionally been rare. One way to work around this limitation is to piece the required data together using time series from sets of similar systems that can be seen as replicates. This can be done in a controlled setting, such as lab experiments to analyze the resilience of fluctuating *Daphnia* populations (*70*). Analogously, in natural situations we may take a space-for-time substitution approach (*71*). For instance, using massive remote sensing data, one can observe changes in tree cover reflecting shifts between tropical forests and savannas, considered to represent alternative attractors with resilience of each of the states depending on climatic conditions (*2*, *67*). Data limitations may sometimes also be ameliorated by adding information about the system based on prior knowledge. For instance, one can make assumptions about the shape of the noise function (e.g., additive noise) and about the shape of the drift function (e.g., polynomials) (*51*) or use mechanistic system knowledge to create realistic models with integrated stochasticity.

Despite challenges yet to be overcome, the mean exit time will be an attractive measure for ecosystem managers. The expected lifetime of a coral reef or tropical forest is an intuitive resilience measure. Methodological and technological advances are increasingly providing high-quality data for systems with tipping points as various as the human body (*72*) and mind (*8*, *73*), financial markets (*9*, *74*), the climate (*75*), and ecosystems (*50*, *67*, *76*). This makes accurate estimations of mean exit time increasingly feasible.

REFERENCES AND NOTES

1. M. Scheffer, S. Carpenter, J. A. Foley, C. Folke, B. Walker, Catastrophic shifts in ecosystems. *Nature* **413**, 591–596 (2001). doi: 10.1038/35098000; pmid: 11595939
2. M. Hirota, M. Holmgren, E. H. Van Nes, M. Scheffer, Global resilience of tropical forest and savanna to critical transitions. *Science* **334**, 232–235 (2011). doi: 10.1126/science.1210657; pmid: 21998390
3. A. C. Staver, S. Archibald, S. A. Levin, The global extent and determinants of savanna and forest as alternative biome states. *Science* **334**, 230–232 (2011). doi: 10.1126/science.1210465; pmid: 21998389
4. T. P. Hughes *et al*., Coral reefs in the Anthropocene. *Nature* **546**, 82–90 (2017). doi: 10.1038/nature22901; pmid: 28569801
5. M. Scheffer, *Ecology of Shallow Lakes* (Chapman and Hall, ed. 1, 1998).
6. S. R. Carpenter, *Regime Shifts in Lake Ecosystems: Pattern and Variation* (Ecology Institute, Oldendorf/Luhe, Germany, 2003).
7. M. Scheffer, *Critical Transitions in Nature and Society* (Princeton Univ. Press, 2009).
8. I. A. van de Leemput *et al*., Critical slowing down as early warning for the onset and termination of depression. *Proc. Natl. Acad. Sci. U.S.A.* **111**, 87–92 (2014). doi: 10.1073/pnas.1312114110; pmid: 24324144
9. S. Battiston *et al*., Complexity theory and financial regulation. *Science* **351**, 818–819 (2016). doi: 10.1126/science.aad0299; pmid: 26912882
10. T. M. Lenton *et al*., Tipping elements in the Earth's climate system. *Proc. Natl. Acad. Sci. U.S.A.* **105**, 1786–1793 (2008). doi: 10.1073/pnas.0705414105; pmid: 18258748
11. M. Scheffer *et al*., Anticipating critical transitions. *Science* **338**, 344–348 (2012). doi: 10.1126/science.1225244; pmid: 23087241
12. C. Folke *et al*., Resilience thinking: Integrating resilience, adaptability and transformability. *Ecol. Soc.* **15**, art20 (2010). doi: 10.5751/ES-03610-150420
13. C. S. Holling, Resilience and stability of ecological systems. *Annu. Rev. Ecol. Syst.* **4**, 1–23 (1973). doi: 10.1146/annurev.es.04.110173.000245
14. M. Scheffer *et al*., Quantifying resilience of humans and other animals. *Proc. Natl. Acad. Sci. U.S.A.* **115**, 11883–11890 (2018). doi: 10.1073/pnas.1810630115; pmid: 30373844
15. M. G. M. Olde Rikkert *et al*., Slowing Down of Recovery as Generic Risk Marker for Acute Severity Transitions in Chronic Diseases. *Crit. Care Med.* **44**, 601–606 (2016). doi: 10.1097/CCM.0000000000001564; pmid: 26765499
16. H. Held, T. Kleinen, Detection of climate system bifurcations by degenerate fingerprinting. *Geophys. Res. Lett.* **31**, L23207 (2004). doi: 10.1029/2004GL020972
17. K. Nyborg *et al*., Social norms as solutions. *Science* **354**, 42–43 (2016). doi: 10.1126/science.aaf8317; pmid: 27846488
18. T. Homer-Dixon *et al*., Synchronous failure: The emerging causal architecture of global crisis. *Ecol. Soc.* **20**, art6 (2015). doi: 10.5751/ES-07681-200306
19. A. R. Ives, B. Dennis, K. L. Cottingham, S. R. Carpenter, Estimating community stability and ecological interactions from time-series data. *Ecol. Monogr.* **73**, 301–330 (2003). doi: 10.1890/0012-9615(2003)073[0301:ECSAEI]2.0.CO;2
20. M. Scheffer *et al*., Early-warning signals for critical transitions. *Nature* **461**, 53–59 (2009). doi: 10.1038/nature08227; pmid: 19727193
21. C. Wissel, A universal law of the characteristic return time near thresholds. *Oecologia* **65**, 101–107 (1984). doi: 10.1007/BF00384470; pmid: 28312117
22. V. Dakos *et al*., Methods for detecting early warnings of critical transitions in time series illustrated using simulated ecological data. *PLOS ONE* **7**, e41010 (2012). doi: 10.1371/journal.pone.0041010; pmid: 22815897
23. S. R. Carpenter, W. A. Brock, Rising variance: A leading indicator of ecological transition. *Ecol. Lett.* **9**, 311–318 (2006). doi: 10.1111/j.1461-0248.2005.00877.x; pmid: 16958897
24. O. N. Bjørnstad, B. T. Grenfell, Noisy clockwork: Time series analysis of population fluctuations in animals. *Science* **293**, 638–643 (2001). doi: 10.1126/science.1062226; pmid: 11474099
25. B. C. Nolting, K. C. Abbott, Balls, cups, and quasi-potentials: Quantifying stability in stochastic systems. *Ecology* **97**, 850–864 (2016). doi: 10.1890/15-1047.1; pmid: 27220202
26. C. W. Gardiner, *Handbook of Stochastic Methods for Physics, Chemistry and the Natural Sciences* (Springer, ed. 3, 2004).
27. M. Scheffer, S. R. Carpenter, V. Dakos, E. H. Van Nes, Generic Indicators of Ecological Resilience: Inferring the Chance of a Critical Transition. *Annu. Rev. Ecol. Evol. Syst.* **46**, 145–167 (2015). doi: 10.1146/annurev-ecolsys-112414-054242
28. F. B. Hanson, H. C. Tuckwell, Persistence times of populations with large random fluctuations. *Theor. Popul. Biol.* **14**, 46–61 (1978). doi: 10.1016/0040-5809(78)90003-5; pmid: 741396
29. See supplementary materials.
30. W. Horsthemke, R. Lefever, *Noise-Induced Transitions: Theory and Applications in Physics, Chemistry, and Biology* (Springer, 1984).
31. M. W. Goldblatt, Vesical tumours induced by chemical compounds. *Br. J. Ind. Med.* **6**, 65–81 (1949). pmid: 18119364
32. B. Ottino-Loffler, J. G. Scott, S. H. Strogatz, Evolutionary dynamics of incubation periods. *eLife* **6**, e30212 (2017). doi: 10.7554/eLife.30212; pmid: 29266000
33. P. E. Sartwell, The incubation period and the dynamics of infectious disease. *Am. J. Epidemiol.* **83**, 204–206 (1966). doi: 10.1093/oxfordjournals.aje.a120576; pmid: 5930773
34. Y. Bakhtin, Universal Statistics of Incubation Periods and Other Detection Times via Diffusion Models. *Bull. Math. Biol.* **81**, 1070–1088 (2019). doi: 10.1007/s11538-018-00558-w; pmid: 30560441
35. T. A. Driscoll, N. Hale, L. N. Trefethen, *Chebfun Guide* (Pafnuty, Oxford, 2014).
36. F. Böttcher *et al*., Reconstruction of complex dynamical systems affected by strong measurement noise. *Phys. Rev. Lett.* **97**, 090603 (2006). doi: 10.1103/PhysRevLett.97.090603; pmid: 17026351
37. R. Friedrich *et al*., Extracting model equations from experimental data. *Phys. Lett. A* **271**, 217–222 (2000). doi: 10.1016/S0375-9601(00)00334-0
38. P. Rinn, P. G. Lind, M. Wachter, J. Peinke, The Langevin approach: An R package for modeling Markov processes. *J. Open Res. Softw.* **4**, e34 (2016). doi: 10.5334/jors.123
39. S. Siegert, R. Friedrich, J. Peinke, Analysis of data sets of stochastic systems. *Phys. Lett. A* **243**, 275–280 (1998). doi: 10.1016/S0375-9601(98)00283-7
40. S. Siegert, R. Friedrich, Modeling of nonlinear Lévy processes by data analysis. *Phys. Rev. E* **64**, 041107 (2001). doi: 10.1103/PhysRevE.64.041107; pmid: 11690010
41. R. M. May, Thresholds and breakpoints in ecosystems with a multiplicity of stable states. *Nature* **269**, 471–477 (1977). doi: 10.1038/269471a0
42. D. Ludwig, D. D. Jones, C. S. Holling, Qualitative analysis of insect outbreak systems the spruce budworm and forest. *J. Anim. Ecol.* **47**, 315–332 (1978). doi: 10.2307/3939
43. S. J. Lade, Finite sampling interval effects in Kramers-Moyal analysis. *Phys. Lett. A* **373**, 3705–3709 (2009). doi: 10.1016/j.physleta.2009.08.029
44. S. R. Carpenter *et al*., Stochastic dynamics of Cyanobacteria in long-term high-frequency observations of a eutrophic lake. *Limnol. Oceanogr.* **5**, 331–336 (2020). doi: 10.1002/lol2.10152
45. C. R. Fragoso Jr.., D. M. L. M. Marques, W. Collischonn, C. E. M. Tucci, E. H. van Nes, Modelling spatial heterogeneity of phytoplankton in Lake Mangueira, a large shallow subtropical lake in South Brazil. *Ecol. Modell.* **219**, 125–137 (2008). doi: 10.1016/j.ecolmodel.2008.08.004
46. W. Dansgaard *et al*., Evidence for general instability of past climate from a 250-kyr ice-core record. *Nature* **364**, 218–220 (1993). doi: 10.1038/364218a0
47. W. S. Broecker, D. M. Peteet, D. Rind, Does the ocean-atmosphere system have more than one stable mode of operation? *Nature* **315**, 21–26 (1985). doi: 10.1038/315021a0
48. P. D. Ditlevsen, Observation of α-stable noise induced millennial climate changes from an ice-core record. *Geophys. Res. Lett.* **26**, 1441–1444 (1999). doi: 10.1029/1999GL900252
49. K. Fuhrer, A. Neftel, M. Anklin, V. Maggi, Continuous measurements of hydrogen peroxide, formaldehyde, calcium and ammonium concentrations along the new grip ice core from summit, Central Greenland. *Atmos. Environ. A* **27**, 1873–1880 (1993). doi: 10.1016/0960-1686(93)90292-7
50. L. Lahti, J. Salojärvi, A. Salonen, M. Scheffer, W. M. de Vos, Tipping elements in the human intestinal ecosystem. *Nat. Commun.* **5**, 4344 (2014). doi: 10.1038/ncomms5344; pmid: 25003530
51. V. N. Livina, F. Kwasniok, T. M. Lenton, Potential analysis reveals changing number of climate states during the last 60 kyr. *Clim. Past* **6**, 77–82 (2010). doi: 10.5194/cp-6-77-2010
52. M. G. Turner, Disturbance and landscape dynamics in a changing world. *Ecology* **91**, 2833–2849 (2010). doi: 10.1890/10-0097.1; pmid: 21058545
53. A. Hastings *et al*., Transient phenomena in ecology. *Science* **361**, eaat6412 (2018). doi: 10.1126/science.aat6412; pmid: 30190378

Downloaded from https://www.science.org at University of British Columbia on September 10, 2021

54. J. H. Connell, Diversity in tropical rain forests and coral reefs. *Science* **199**, 1302–1310 (1978). doi: 10.1126/science.199.4335.1302; pmid: 17840770
55. G. W. A. Constable, T. Rogers, A. J. McKane, C. E. Tarnita, Demographic noise can reverse the direction of deterministic selection. *Proc. Natl. Acad. Sci. U.S.A.* **113**, E4745–E4754 (2016). doi: 10.1073/pnas.1603693113; pmid: 27450085
56. Y. A. Kuznetsov, *Elements of Applied Bifurcation Theory* (Springer, 1995).
57. G. J. E. Santos, M. Rivera, M. Eiswirth, P. Parmananda, Effects of noise near a homoclinic bifurcation in an electrochemical system. *Phys. Rev. E* **70**, 021103 (2004). doi: 10.1103/PhysRevE.70.021103; pmid: 15447475
58. T. S. Eaves, N. J. Balmforth, Noisy homoclinic pulse dynamics. *Chaos* **26**, 043104 (2016). doi: 10.1063/1.4945794; pmid: 27131483
59. E. Benincà, V. Dakos, E. H. Van Nes, J. Huisman, M. Scheffer, Resonance of plankton communities with temperature fluctuations. *Am. Nat.* **178**, E85–E95 (2011). doi: 10.1086/661902; pmid: 21956036
60. V. Dakos *et al.*, Interannual variability in species composition explained as seasonally entrained chaos. *Proc. R. Soc. B* **276**, 2871–2880 (2009). doi: 10.1098/rspb.2009.0584; pmid: 19474038
61. D. W. Hosmer, S. Lemeshow, S. May, *Applied Survival Analysis: Regression Modeling of Time-to-Event Data* (Wiley, 2011).
62. F. Hassanibesheli, N. Boers, J. Kurths, Reconstructing complex system dynamics from time series: A method comparison. *New J. Phys.* **22**, 073053 (2020). doi: 10.1088/1367-2630/ab9ce5
63. W. Just, K. Gelfert, N. Baba, A. Riegert, H. Kantz, Elimination of Fast Chaotic Degrees of Freedom: On the Accuracy of the Born Approximation. *J. Stat. Phys.* **112**, 277–292 (2003). doi: 10.1023/A:1023635805818
64. R. Friedrich, J. Peinke, M. Sahimi, M. Reza Rahimi Tabar, Approaching complexity by stochastic methods: From biological systems to turbulence. *Phys. Rep.* **506**, 87–162 (2011). doi: 10.1016/j.physrep.2011.05.003
65. V. Lucarini, D. Faranda, M. Willeit, Bistable systems with stochastic noise: Virtues and limits of effective one-dimensional Langevin equations. *Nonlinear Process. Geophys.* **19**, 9–22 (2012). doi: 10.5194/npg-19-9-2012
66. V. Dakos *et al.*, Slowing down as an early warning signal for abrupt climate change. *Proc. Natl. Acad. Sci. U.S.A.* **105**, 14308–14312 (2008). doi: 10.1073/pnas.0802430105; pmid: 18787119
67. J. Verbesselt *et al.*, Remotely sensed resilience of tropical forests. *Nat. Clim. Chang.* **6**, 1028–1031 (2016). doi: 10.1038/nclimate3108
68. F. Bouchet, J. Reygner, Generalisation of the Eyring-Kramers Transition Rate Formula to Irreversible Diffusion Processes. *Ann. Henri Poincare* **17**, 3499–3532 (2016). doi: 10.1007/s00023-016-0507-4
69. A. Bovier, M. Eckhoff, V. Gayrard, M. Klein, Metastability in reversible diffusion processes I. Sharp asymptotics for capacities and exit times. *J. Eur. Math. Soc.* **6**, 399–424 (2004). doi: 10.4171/JEMS/14
70. J. M. Drake, B. D. Griffen, Early warning signals of extinction in deteriorating environments. *Nature* **467**, 456–459 (2010). doi: 10.1038/nature09389; pmid: 20827269
71. S. T. A. Pickett, in *Long-Term Studies in Ecology: Approaches and Alternatives*, G. E. Likens, Ed. (Springer, 1989), pp. 110–135.
72. S. M. W. Gijzel *et al.*, Dynamical indicators of resilience in postural balance time series are related to successful aging in high-functioning older adults. *J. Gerontol. A* **74**, 1119–1126 (2019). doi: 10.1093/gerona/gly170; pmid: 30052796
73. M. Wichers, P. C. Groot, Critical slowing down as a personalized early warning signal for depression. *Psychother. Psychosom.* **85**, 114–116 (2016). doi: 10.1159/000441458; pmid: 26821231
74. D. Sornette, R. Woodard, in *Econophysics Approaches to Large-Scale Business Data and Financial Crisis*, M. Takayasu, T. Watanabe, H. Takayasu, Eds. (Springer, 2010), pp. 101–148.
75. T. M. Lenton, V. Dakos, S. Bathiany, M. Scheffer, Observed trends in the magnitude and persistence of monthly temperature variability. *Sci. Rep.* **7**, 5940 (2017). doi: 10.1038/s41598-017-06382-x; pmid: 28725011
76. F. Müller, C. Baessler, H. Schubert, S. Klotz, *Long-Term Ecological Research: Between Theory and Application* (Springer, 2010).
77. P. Massart, The Tight Constant in the Dvoretzky-Kiefer-Wolfowitz Inequality. *Ann. Probab.* **18**, 1269–1283 (1990). doi: 10.1214/aop/1176990746
78. A. Dvoretzky, J. Kiefer, J. Wolfowitz, Asymptotic Minimax Character of the Sample Distribution Function and of the Classical Multinomial Estimator. *Ann. Math. Stat.* **27**, 642–669 (1956). doi: 10.1214/aoms/1177728174

ACKNOWLEDGMENTS

Funding: Lake Mendota data were collected by the North Temperate Lakes Long-Term Ecological Research Program funded by NSF grant DEB-1440297. This study was carried out under the program of the Netherlands Earth System Science Centre (NESSC; 024.002.001). L.L. was supported by Academy of Finland (decisions 295741 and 330887). **Author contributions:** B.M.S.A., conceptualization, methodology, writing–original draft, data curation, formal analysis; S.R.C. and L.L., data curation; E.H.v.N., methodology, visualization, software; M.S., conceptualization; all authors, writing–review and editing. **Competing interests:** The authors have no competing interests. **Data and materials availability:** All data and code are available in the supplementary materials.

SUPPLEMENTARY MATERIALS

science.sciencemag.org/content/372/6547/eaay4895/suppl/DC1
Movies S1 and S2
MATLAB code
References (*79*–*90*)

23 June 2019; resubmitted 20 August 2020
Accepted 28 April 2021
10.1126/science.aay4895

Downloaded from https://www.science.org at University of British Columbia on September 10, 2021

Science

Exit time as a measure of ecological resilience

Babak M. S. AraniStephen R. CarpenterLeo LahtiEgbert H. van NesMarten Scheffer

Science, 372 (6547), eaay4895.

Estimating resilience in complex systems
Resilience is an important concept in the study of critical transitions and tipping points in complex systems and is defined by the size of the disturbance that a system can endure before tipping into an alternative stable state. Nevertheless, resilience has proved resistant to measurement. Arani *et al.* show how the mathematical concept of mean exit time, the time it takes for a system to cross a threshold, can help to solve this problem and characterize the resilience of complex systems. They derived a model approach to estimate exit time from time series data and applied it to examples from a grazed plant population model, lake cyanobacterial data, and Pleistocene-Holocene climate data. This approach may improve our understanding of the dynamical properties of complex systems under threat.

Science, aay4895, this issue p. eaay4895

View the article online
https://www.science.org/doi/10.1126/science.aay4895
Permissions
https://www.science.org/help/reprints-and-permissions

Downloaded from https://www.science.org at University of British Columbia on September 10, 2021

Use of think article is subject to the Terms of service

Science (ISSN 1095-9203) is published by the American Association for the Advancement of Science. 1200 New York Avenue NW, Washington, DC 20005. The title *Science* is a registered trademark of AAAS.
Copyright © 2021 The Authors, some rights reserved; exclusive licensee American Association for the Advancement of Science. No claim to original U.S. Government Works